Published in final edited form as:
Radiology. 1990 December ; 177(3): 769–772.

Myocardial Tagging in Polar Coordinates with Use of Striped Tags[1]

Bradley D. Bolster Jr, B EE, **Elliot R. McVeigh, PhD**, and **Elias A. Zerhouni, MD**
Departments of Biomedical Engineering (B.D.B.) and Radiology (E.R.M., E.A.Z.), The Johns Hopkins University, 600 N Wolfe St. Baltimore, MD 21205.

Abstract

Regional deformation abnormalities in the heart wall provide a good indicator of ischemia. Myocardial tagging with magnetic resonance imaging is a new method of assessing heart wall motion during contraction. Current methods of myocardial tagging either do not provide two-dimensional information or lack a coordinate system well adapted to the morphology of the heart. In this article, the authors describe a new tagging method that provides a true polar coordinate system, with both radial and angular dimensions. This is accomplished with use of a section-selective version of spatially modulated magnetization resulting in striped tags (STAGs). These STAG planes are placed in the myocardium in a star pattern so that they intersect on the long axis of the heart and stripes appear through the width of the heart wall. In the short-axis view during contraction, rotation around the long axis yields angular information such as shear and twist, while separation of the stripes within the myocardium permits measurement of radial thickening. Therefore, this method provides a coordinate system for calculating two-dimensional strain that is adapted to the morphology of the left ventricle.

Keywords

Heart, function; Magnetic resonance (MR), physics; Magnetic resonance (MR), technology; Myocardium, MR studies, 511.1214

Abnormalities in regional heart wall deformation are a good indicator of regional ischemia. By assessing this motion, it is possible that ischemia can be detected with higher sensitivity. The motion of the heart during its cycle, however, is very complex. Unless invasive landmarks such as implanted radiopaque markers (1-9) or sonomicrometers (10-13) are used, it is not possible to track specific myocardial points throughout the cardiac cycle with any of the current imaging modalities. As demonstrated by Zerhouni et al (14), tagging of the myocardium with use of magnetic resonance (MR) imaging allows more precise measurement of local and regional myocardial deformation. In the first implementation of this concept, inversion radio-frequency (RF) pulses distributed either radially about the long ventricular axis or parallel to the short axis were used to perturb the magnetization of protons in selected regions of the myocardium (Fig 1a). On subsequent images, obtained in a plane orthogonal to the tagging planes, stripes representing the tagged regions were observed and could be tracked throughout the cardiac cycle. This radial tagging scheme provides a good indication of myocardial twist and shear, but is limited because deformation along a tag can only be measured from the epicardial to the endocardial surface, thus preventing accurate determination of the transmural differences in strain. Strain, in this case, corresponds to the relative motion of defined points in the myocardium produced by the stress occurring during contraction.

Address reprint requests to E.R.M.

More recently, Axel and Dougherty (15) have proposed a different tagging scheme that uses spatially modulated magnetization (SPAMM) to place a tagging grid of longitudinal magnetization disturbance into the myocardium (Fig 1b). The intersection points of this grid can then be tracked through contraction. Although this scheme offers the advantage of imposing a Cartesian grid of points, allowing two-dimensional measures of deformation, the points are distributed at different depths in the myocardial wall.

We propose a new tagging scheme that combines the advantages of both methods. Radial tagging in a polar coordinate system is best suited to the ventricular geometry. Therefore, we use the radial tagging pattern with the added advantage of discrete points within the heart wall. The method presented here is, in effect, a section-selective version of SPAMM, creating striped tags (STAGs).

MATERIALS AND METHODS

Theory

In the preinversion method, sections perpendicular to the imaging plane are selectively excited with a shaped 180° pulse as shown in Figure 2. This results in tagged planes of inverted magnetization that persist in the sample. When images are obtained in planes perpendicular to the tagged planes, the tagged planes appear as lines in the image. For cardiac studies, several tagged planes that have a common line of intersection along the long axis of the heart are produced. In the short-axis image, this results in several lines of differing angles about a center point on the cardiac long axis.

The SPAMM sequence, shown in Figure 3, causes spatially modulated magnetization by exciting the whole sample to a tip angle, Θ, that is usually less than 90°, creating a substantial transverse component to the magnetization vector M. A magnetic field gradient is then applied across the sample, causing the transverse magnetization to dephase linearly across the sample in the direction of the gradient. The phase of the bulk magnetization in the transverse plane can then be described by

$$\Phi(\mathbf{r}) = \gamma \int_{t_1}^{t_2} [\mathbf{G}(t) \cdot \mathbf{r}] \mathrm{d}t,$$

where t_2-t_1 is the duration of the gradient pulse, **G** is the gradient strength vector as a function of time, **r** is the position vector relative to center, and γ is the gyromagnetic ratio. A second excitation pulse is then applied with the same magnitude as the first. The amount of tip angle caused by this pulse is directly proportional to the sine of the angle between the $\mathbf{H}_1$ vector of the RF pulse and the transverse magnetization (the $\mathbf{H}_1$ vector is the direction of the magnetic field caused by the RF in the rotating frame). Therefore, the resulting longitudinal magnetization is given by $\mathbf{M}_z(\mathbf{r}) = -\sin^2(\Theta)\cos[\Phi(\mathbf{r})] + \cos^2(\Theta)$. If Θ 90°, then $\mathbf{M}_z = -\cos[\Phi(\mathbf{r})]$ a sinusoidal distribution of longitudinal magnetization. If the tip angle caused by the second pulse is always 90°,then the amplitude of the sinusoidal variation can be modulated by the sine of the first excitation tip angle. A spoiler is used after this sequence to dephase remaining transverse magnetization. To create a grid pattern, the same sequence is then repeated with an orthogonal magnetic field gradient.

Like the SPAMM sequence, the STAG sequence (Fig 4) spatially modulates magnetization, except it does this in a selected section. The 180° pulses used in the preinversion technique are divided into two 90° section-selective pulses. After the first 90° pulse, a gradient parallel with the imaging plane and orthogonal to the initial section-selection gradient is applied (this is the first y-gradient pulse in Figure 4). This gradient is used to produce a linear phase shift of the transverse magnetization as a function of distance along the tag plane. The second 90° pulse tips or rotates the transverse magnetization about the $\mathbf{H}_1$ vector. Therefore, transverse

magnetization vectors parallel to $\mathbf{H}_1$ remain completely transverse, while magnetization vectors orthogonal to $\mathbf{H}_1$ become longitudinal again. Thus, the linear phase shift along the tag section yields a sinusoidal variation of longitudinal magnetization along the tag between positive and negative $\mathbf{M}_z$. This is described in detail by Axel and Dougherty (15).

Because a gradient was used during the RF tagging pulses (Fig 4), dephasing occurs across the section that defines the tagged plane. The tagged plane needs to be refocused to produce stripes that are orthogonal to the direction of the tag, so a pair of self-refocusing RF pulses are employed. The dephasing caused by the gradient in the first selective 90° pulse is refocused by means of the reversed gradient in the second selective 90° pulse. If the plane being excited is not at the physical center of the gradient, however, the second 90° pulse excites a plane on the opposite side of the center than does the first 90° pulse. The phase shift applied to the second RF pulse by reversing the quadrature channel of the RF counteracts the effect of the reversed gradient, causing the same plane to be excited by both RF pulses.

The sequence shown in Figure 4 may be repeated for several planes to create intersecting STAGs in the imaging plane. Between each tagging set, a spoiler gradient is used to dephase the remaining transverse magnetization and remove the possibility of stimulated echoes in the imaging sequence. After the tags have been created, images can be obtained with a standard spin-echo sequence. Movement of the tags can then be recorded by measuring their position at different intervals from the tagging time.

For a multiphasic study of the heart, the above multitag sequence can be triggered with the upslope of the QRS complex of the electrocardiogram. The tagging sequence is then followed by the imaging sequence, as shown in Figure 5. By acquiring multiple sections and rearranging the order of section acquisition, a multiphasic study can be created for each of the sections acquired.

Experiment

The STAG sequence was implemented with use of a whole-body MR imager (Signa; GE Medical Systems, Milwaukee) operating at 1.5 T. For development and tuning purposes, studies were first performed on water phantoms in the body coil. Attenuation properties of the phantom allowed evaluation of RF strength dependence for the tagging pattern. Use of higher resolution and smaller field of view showed the actual tag pattern in detail.

Multiphasic studies were performed on four healthy volunteers between the ages of 24 and 40 years. Informed consent was obtained from all subjects. These studies were electrocardiographically gated at heart rates between 45 and 75 beats per minute, with six STAGs placed prior to imaging. Images were obtained on a 128 × 256 matrix with a 20-cm field of view. Two averages were used, requiring a total imaging time of approximately 25 minutes. The tags were created at the onset of the QRS complex, and the first image was obtained 28 msec after the QRS. The subsequent two or three images were obtained 90 msec apart. Time resolution can be increased by acquiring another set of images in which the initial image has been offset in time. This new set of images is interleaved with the previous set, thus doubling the time resolution.

RESULTS

In phantoms, the tags appeared as “beads.” The shape and spacing of these tags were not dependent on RF strength. Center-to-center distances as small as 1.7 mm were achieved with use of varying strengths of the phasing gradient pulse. Resolution was limited by the number of phaseencoding steps used in image acquisition. In intersecting tags, the radius of each tag

striping point was consistent from tag to tag (Fig 6). Therefore, a radial coordinate system that fits well with the morphology of the left ventricle could easily be applied to the resulting data.

In the human heart, three- and four-phase studies showed good tag persistence from end diastole to end systole. The phasing gradient pulse was adjusted to yield a point every 3.1 mm. Tagged points closer to the endocardium separated more during contraction than points near the epicardium, which demonstrates that important information about the transmural dependence of myocardial thickening during contraction can be obtained from this technique. STAG images from a human heart are shown at two time points in Figure 7.

DISCUSSION

The contraction of the heart is composed of complex motions including translation, rotation, torsion, shear, and thickening. Information about cardiac dysfunction can be obtained by measuring regional differences in torsion around the cardiac long axis (16-17) and thickening of the myocardial walls (18-19).

A tagging method should measure transmural dependence of myocardial thickening because abnormal thickening of the endocardial half of the myocardium has been shown to be the most sensitive indicator of ischemia (20). The star pattern of tags obtained with the preinversion method is excellent for measuring torsion, but transmural differences in thickening of the myocardium cannot be measured.

The SPAMM grid method creates multiple tagging points in the heart wall, allowing some assessment of transmural thickening, but the resulting points do not occur at the same depth at different locations in the myocardium. This makes direct comparisons of transmural thickening somewhat difficult. At high resolution, interference patterns at the intersections of the two-dimensional grid further complicate analysis.

The STAG method, however, alleviates the problems of both of the above methods. Since the left ventricle is generally ellipsoid in shape, with rotational deformation around the long axis and thickening radial to the long axis, use of a polar coordinate system is most appropriate to assess left ventricular morphology and motion. The STAG method uses the polar coordinate system, in which as many as four radial collinear reference points are placed through the myocardial wall at different angles around the long axis. This provides good resolution for studying the transmural dependence of myocardial thickening and adequate sampling of rotational motion contributing to the measurement of shear.

Acknowledgments

We thank Leon Axel, MD, PhD, Bill Hunter, PhD, and Jerry Prince, PhD, for helpful comments and discussion.

Abbreviations

RF, radio frequency; SPAMM, spatially modulated magnetization; STAG, striped tag.

References

1. Ingels NB, Daughters GT, Stinson EB, Alderman EL. Measurement of midwall myocardial dynamics in intact man by radiography of surgically implanted markers. Circulation 1975;52:859–867. [PubMed: 1175267]
2. Fenton TR, Cherry JM, Klassen GA. Transmural myocardial deformation in the canine left ventricular wall. Am J Physiol 1980;235:319–329.
3. Meier GD, Ziskin MC, Santamore WP, Bove AA. Kinematics of the beating heart. IEEE Trans Biomed Eng 1980;27:319–329. [PubMed: 7390529]

4. Meier GD, Bove AA, Santamore WP. Contractile function in canine right ventricle. Am J Physiol 1980;239:H794–804. [PubMed: 7446754]
5. Ingels NB Jr, Daughters GT 2d, Stinson EB, Alderman EL. Evaluation of methods for quantifying left ventricular segmental wall motion in man using myocardial marker as a standard. Circulation 1980;61:966–972. [PubMed: 6988104]
6. Walley KR, Grover M, Raff GL, Benge W, Hannaford B, Glantz SA. Left ventricular dynamic geometry in the intact and open chest dog. Circ Res 1982;50:573–589. [PubMed: 7067064]
7. Klassen GA, Fenton TR. Transmural myocardial deformation in the canine left ventricle: normal in vivo three-dimensional finite strains. Circ Res 1986;58:310. [PubMed: 3948347]
8. Garrison JB, Ebert WL, Jenkins RE, et al. Measurement of three-dimensional positions and motions of large numbers of spherical radiopaque markers from biplane cineradiograms. Comp Biomed Res 1982;15:76–96.
9. Waldman LK, Fung YC, Covell JO. Transmural myocardial deformation in the canine left ventricle. Circ Res 1985;57:152–163. [PubMed: 4006099]
10. LeWinter MM, Kent RS, Kroener JM, Carew TE, Covell JW. Regional differences in myocardial performance in the left ventricle of the dog. Circ Res 1975;37:191–199. [PubMed: 1149193]
11. Sabbah HN, Marzilli M, Stein PD. The relative role of subendocardium and subepicardium in left ventricular mechanics. Am J Physiol 1981;240:H920–926. [PubMed: 7246754]
12. Gallagher KP, Osakada C, Matsuzaki M, Miller M, Kemper WS, Ross J Jr. Subepicardial segmental function during coronary stenosis and the role of myocardial fiber orientation. Circ Res 1982;50:352–359. [PubMed: 7060231]
13. Myers JH, Stirling MC, Choy M, Buda AJ, Gallagher KP. Direct measurement of inner and outer wall thickening dynamics with epicardial echocardiography. Circulation 1986;74:164–172. [PubMed: 3708771]
14. Zerhouni EA, Parish DM, Rogers WJ, Yang A, Shapiro EP. Human heart: tagging with MR imaging-a method for noninvasiye assessment of myocardial motion. Radiology 1988;169:59–63. [PubMed: 3420283]
15. Axel L, Dougherty L. MR imaging of motion with spatial modulation of magnetization. Radiology 1989;171:841–845. [PubMed: 2717762]
16. Buchalter MB, Weiss JL, Rogers WJ, et al. Noninvasive quantification of left ventricular twist and torsion in normal humans using magnetic resonance myocardial tagging. Circulation 1990;81:1236–1244. [PubMed: 2317906]
17. Shapiro EP, Buchalter MB, Rogers WJ, Zerhouni EA, Guier WH, Weiss JL. LV twist is greater with inotropic stimulation and less with regional ischemia. Circulation 1988;78(suppl 2):466.
18. Lima J, Weiss J, Lessick J, et al. Dysfunction of the adjacent nonischemic zone: is end-systolic stress increased (abstr)? Circulation 1989;80(suppl 2):97.
19. Lima J, Bouton S, Zerhouni E, et al. Nonischemic adjacent dysfunction is greatest in the subendocardium during ischemia (abstr). Circulation 1989;80(suppl 2):97.
20. Gallagher KP, Osakada G, Matsuzaki M, et al. Nonuniformity of inner and outer systolic wall thickening in conscious dogs. Am J Physiol 1985;248:H241. [PubMed: 4025560]

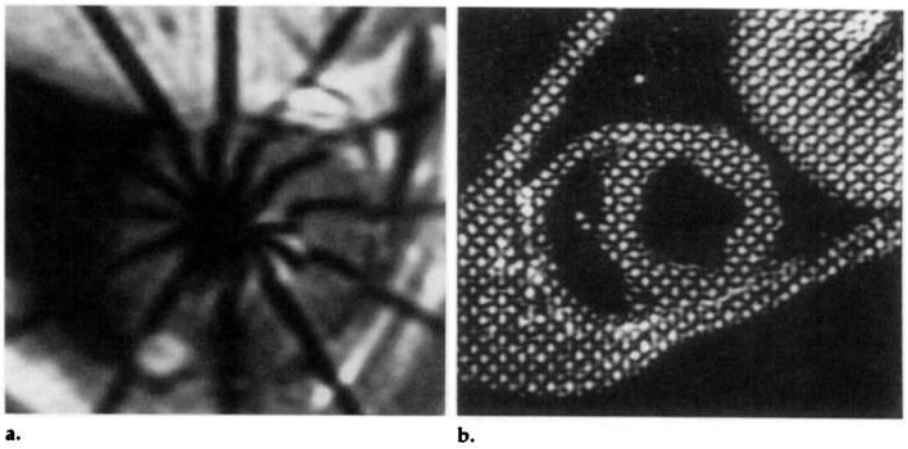

Figure 1.
(a) MR image of canine left ventricle tagged with the preinversion pulse sequence. The line of intersection of the tag planes occurs along the long axis of the heart. **(b)** MR image of a canine heart tagged with the SPAMM sequence to create an orthogonal grid. Resolution allows one to three intersecting lines in the heart wall.

Figure 2.
The preinversion pulse sequence. The RF inversion pulses are section selective. The angle of each tag plane is set by the x and y gradients (*XGRAD* and *YGRAD*), which, in this case, rotate in the tag plane.

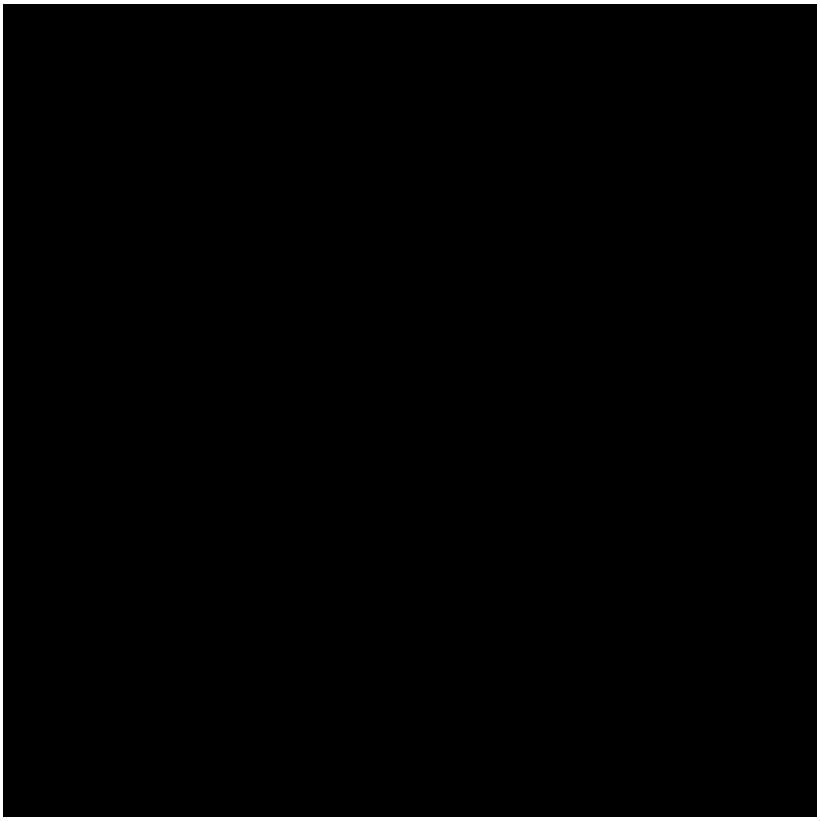

Figure 3.
The one-dimensional SPAMM sequence. The first RF pulse excites the whole sample with a 90° pulse. The gradient pulse then provides a phase shift in the transverse magnetization that is linearly dependent on position. The second RF pulse results in a longitudinal component of magnetization that sinusoidally varies with position. The spoiler pulse cancels signal from the remaining transverse magnetization.

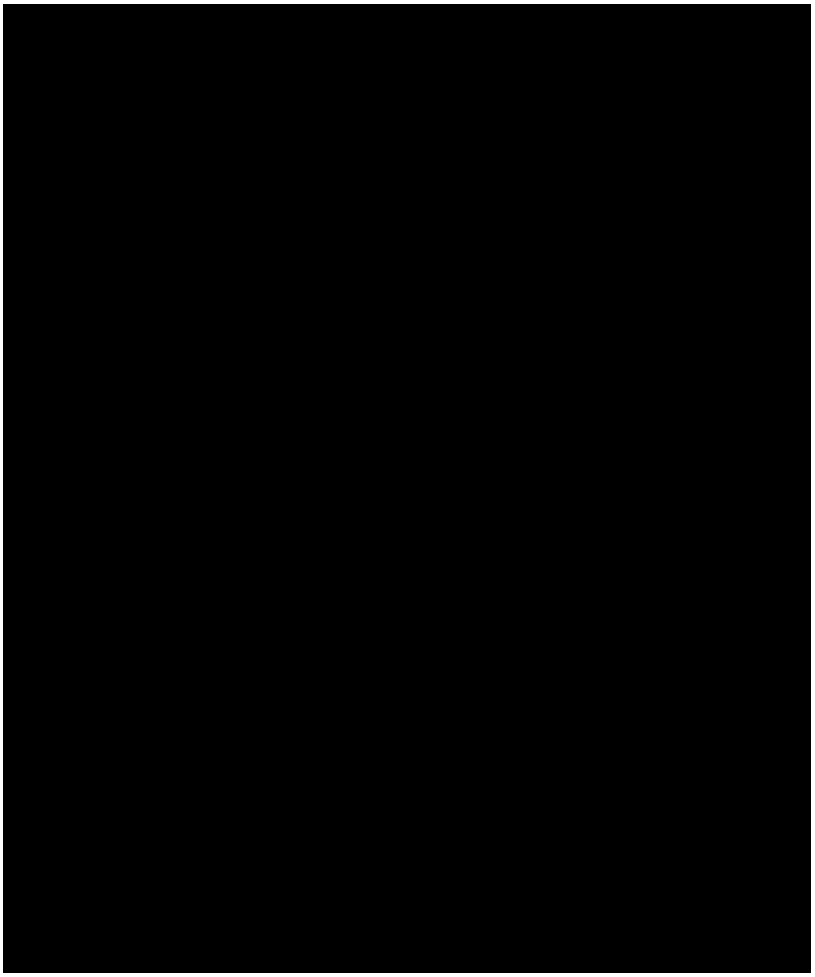

Figure 4.
The STAG pulse sequence. A phasing gradient is used after the first 90° section-selective pulse to linearly distribute the transverse phase in a direction along the selected section. The second 90°pulse rotates this transverse magnetization, with the magnitude of the longitudinal component dependent on the previous phase in the transverse plane. The spoiler pulses disperse any remaining transverse magnetization. *RFI* = in-phase channel of the RF, *RFQ* = the quadrature of the RF, *XGRAD* = x gradient, *YGRAD* = y gradient.

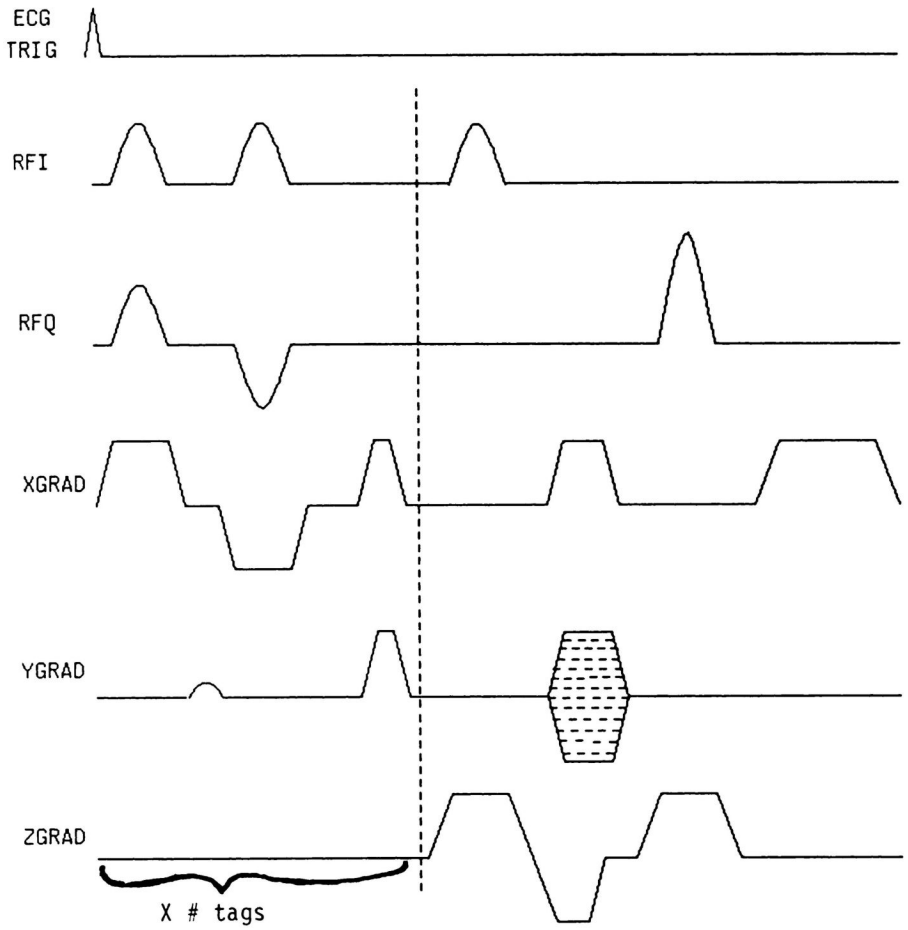

Figure 5.
The STAG sequence is followed by a standard spin-echo imaging sequence. The beginning of the tagging sequence is gated by the upslope of the QRS complex. The tagging sequence is repeated at different angles for each STAG and the imaging sequence can be repeated at different delays after tagging to measure motion. *ECG TRIG* = electrocardiographic triggering, *RFI* = in-phase channel of the RF, *RFQ* = the quadrature of the RF, *XGRAD* = x gradient, *YGRAD* = y gradient, *ZGRAD* = z gradient.

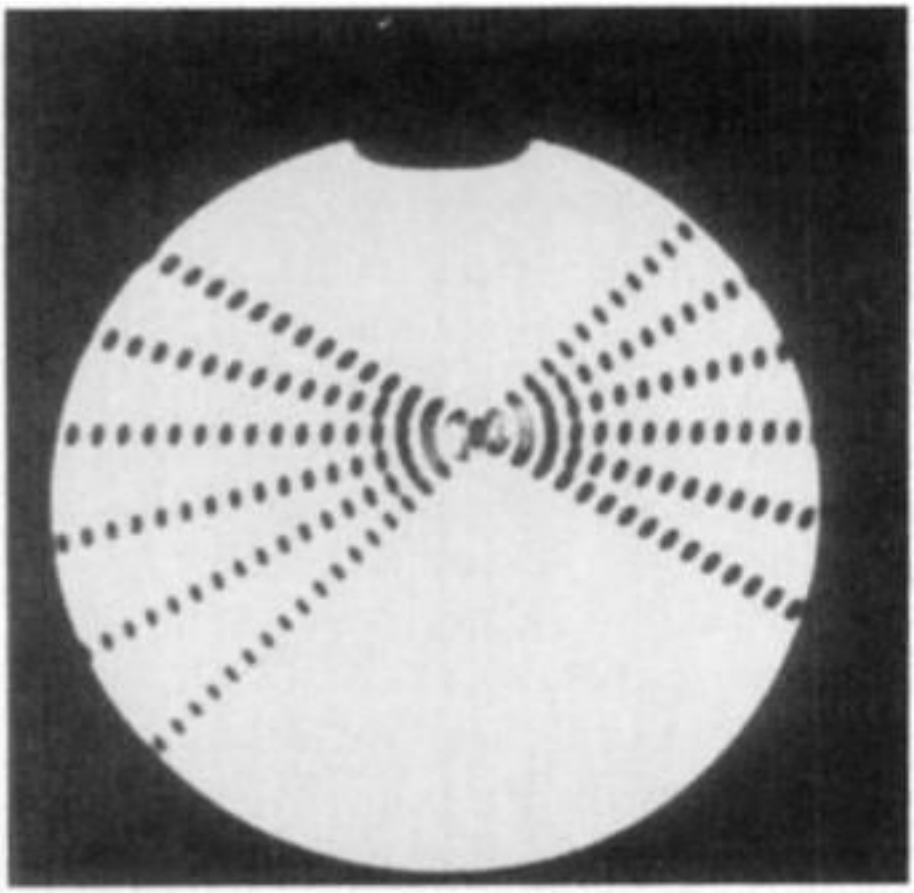

Figure 6.
MR image obtained with use of the STAG sequence of a 1-L water phantom. The quadrature head coil and a 16-cm field of view were used. The angular separation of the tags is reduced in this example to show the coherence in the sinusoidal striping in the tags. This effectively sets up a polar coordinate system.

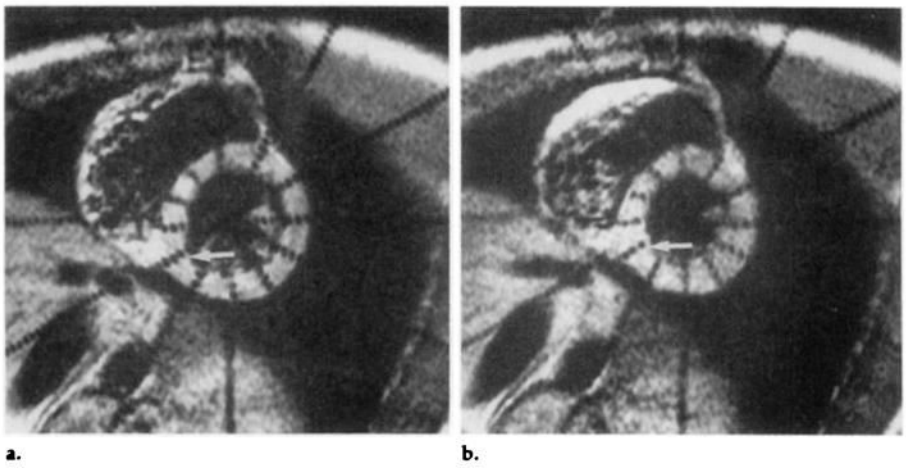

Figure 7.
MR images of a human heart obtained with use of the STAG sequence. Images were obtained 90 msec apart, with short-axis views centered on the long axis. Here, a 20-cm field of view was used and as many as four tag points occurred in the myocardial wall. As the heart contracts —**a** to **b**—points closer to the endocardium separate more than the epicardial points (arrow), demonstrating transmural dependence of wall thickening.